Lateral Control of an Autonomous Vehicle

Jingjing Jiang[1] and Alessandro Astolfi[2]

***Abstract*—The asymptotic stabilization problem for a class of nonlinear under-actuated systems is studied and solved. Its solution, together with the back-stepping and the forwarding control design methods, is exploited in the control of the nonlinear lateral dynamics of a vehicle. Even though the theoretical studies of the lateral control of autonomous vehicles are traditionally applied to lane keeping cases, the results can be applied to broader range of areas, such as lane changing cases. The comparison between the performances of the closed-loop systems with the given controller and a typical human driver is given and demonstrates the speediness and the effectiveness of the feedback controller.**

NOMENCLATURE

β	ratio of the lateral speed and the longitudinal speed
$\dot{\psi}$	yaw rate [rad/s]
ψ_L	heading error, relative yaw angle [rad]
δ	actual steering angle [rad]
δ_d	steering angle at the column system [rad]
ρ	road curvature $[\mathrm{m}^{-1}]$
η_t	width of the tyre contact patch [m]
a_y	lateral acceleration of the car $[\mathrm{m} \times \mathrm{s}^{-2}]$
B_u	damping coefficient of the steering system $[\mathrm{Nm}/(\mathrm{rad} \times \mathrm{s})]$
$C_f(C_r)$	front (rear) tyre cornering stiffness [N/rad]
$F_f(F_r)$	front (rear) tyre lateral force [N]
I_z	moment inertia of the car about the yaw-axis $[\mathrm{kg} \times \mathrm{m}^2]$
J_s	moment of inertia of the steering system $[\mathrm{kg} \times \mathrm{m}^2]$
K_a	visual anticipatory control of the driver
K_c	proportional gain of the transfer function representing the compensatory steering control of the driver
$l_f(l_r)$	distances of the front (rear) tyres to the mass center [m]
m	mass of the car [kg]
R_s	reduction ratio of the steering system, *i.e.* $R_s = \delta_d/\delta$
T_c	torque generated by the controller [Nm]
$T_i(T_l)$	lag (lead) time constant of the transfer function representing the compensatory steering control of the driver
T_n	neuromuscular lag time constant of the driver
T_p	driver's preview time [s]
T_s	self-aligning moment of the steering system [Nm]
v_x	longitudinal speed of the car [m/s]
v_y	lateral speed of the car [m/s]
y_L	lateral deviation of the car [m]

[1]J. Jiang is with the Department of Electrical and Electronic Engineering, Imperial College London, UK, E-mail: jingjing.jiang10@imperial.ac.uk

[2]A. Astolfi is with the Dept. of Electrical and Electronic Engineering, Imperial College London, London, SW7 2AZ, UK and the DICII, University of Roma "Tor Vergata", Via del Politecnico 1, 00133 Rome, Italy, E-mail: a.astolfi@imperial.ac.uk

I. INTRODUCTION

The study on auto-driving cars is a rapidly growing research area. Many companies across the world, such as Google®and Tesla®, are investing millions of dollars in the development of self-driving autonomous cars. Compared with traditional cars controlled completely by the human driver and the cars with passive shared-controller (*e.g. anti-skid brake system (ABS)*), self-driving cars have the following advantages: the number of car accidents could be reduced drastically and thousands of lives saved; traffic congestions can be significantly reduced and energy efficiency can be greatly improved; people can spend their commuting time on other more valuable things; it is more convenient for the elderly, the children and the disabled to use cars.

To achieve autonomous driving along a pre-defined trajectory, such as a route planned by Google Map®from the house where you live to the place where you work, the control problems for the longitudinal and lateral dynamics of the vehicle have to be studied and solved. Even though the longitudinal dynamics and the lateral dynamics of the vehicle are coupled, it is common to assume that the two are decoupled whenever the road curvature is small [1]. The paper [2] has investigated the control of vehicle longitudinal dynamics, while this paper focuses on the control of the lateral dynamics.

The lateral dynamics of vehicles has been discussed in [3], in which the kinematic and the dynamic models for lateral vehicle motion have been studied. Many control schemes have been established to control the lateral dynamics. The papers [4] and [5] have proposed control laws based on Proportional–Integral–Derivative (PID) control, while the paper [6] has developed a lateral controller based on fuzzy control. Other control technologies have also been used, such as H_∞ control [7], [8], Linear Quadratic Regulator (LQR) [9] and sliding mode control [10], [11], [12]. In addition, the paper [13] has presented a feedback controller to control the lateral dynamics of rear-wheel drive cars subject to state constraints. However, these control methods are developed based on the linearized model of the lateral dynamics, while this paper studies the control problem for the nonlinear lateral dynamics. Model Predictive Control (MPC) is another method used in the trajectory tracking of autonomous cars, for example [14], [15], [16]. The computation time of nonlinear MPC is the main disadvantage of such an approach: this paper proposes an analytical solution to the lateral control problem which does not

cause any computation burdens. Finally, the papers [17], [18] have studied the lateral control of independently actuated four-wheeled vehicles. Comparisons of different lateral controllers can be found in [19], [20].

The main contributions of the paper are stated as follows. The paper studies the asymptotic stabilization problem for a class of nonlinear systems and exploits the solution to solve the lateral control problem. A Lyapunov-like analysis is used to prove the stability of the closed-loop system.

This paper is organized as follows. Section II describes the model we study in the paper and formulates the lateral control problem for autonomous vehicles. Some preliminary theorems which are essential to design the lateral controller are presented and proved in Section III, while the solution to the lateral control problem is given in Section IV, in which formal properties of the closed-loop system are presented. Section V studies three examples and shows how the controller works in different cases. By comparing the simulation results with typical driver performances we demonstrate the effectiveness of the established controller. Finally, conclusions and suggestions for future work are given in Section VI.

II. SYSTEM MODELING AND PROBLEM STATEMENT

Assumption 1: We assume that the longitudinal speed is constant, *i.e.* v_x is a constant, and strictly positive.

Based on the well-known Newton's Second Law for motion along the lateral axis we have

$$ma_y = F_f + F_r,$$

where a_y denotes the lateral acceleration of the car, F_f and F_r represent the lateral tyre forces of the front and rear wheels, respectively. The lateral acceleration is caused by the motion along the lateral axis (*i.e.* the y-axis) and the centripetal acceleration $v_x\dot{\psi}$, where v_x and $\dot{\psi}$ are the longitudinal speed of the car and the yaw rate, respectively. Hence, the lateral translational motion can be described as

$$m(\dot{v}_y + v_x\dot{\psi}) = F_f + F_r, \tag{1}$$

where m is the mass of the car. In addition, the moment balance about the vertical axis yields the equation for the yaw dynamics

$$I_z\ddot{\psi} = F_f l_f - F_r l_r, \tag{2}$$

where I_z denotes the moment of inertia of the car about the yaw-axis, and l_f and l_r represent the distances of the front tyre and the rear tyre to the vehicle mass center, respectively.

The side-slip angles for the front and the rear wheels of the car, α_f and α_r, are defined in Fig. 1, where v denotes the velocity of the vehicle, *i.e.* v is the combination of the longitudinal speed v_x and the lateral speed v_y, and δ is the steering angle. In addition, θ_f and θ_r represent the angles between the velocity vector v and the longitudinal speed direction, respectively, and can be calculated as

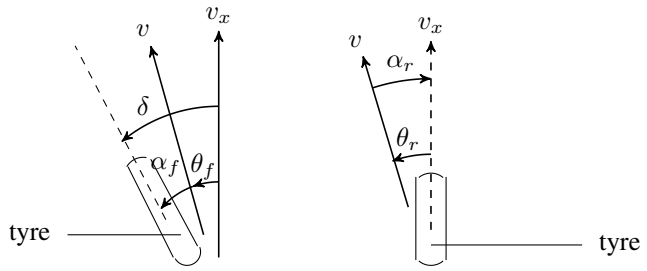

(a) Front Tyre Side-Slip Angle (b) Rear Tyre Side-Slip Angle

Fig. 1: Definitions of Tyre Side-Slip Angles

$$\tan(\theta_f) = \frac{v_y + l_f\dot{\psi}}{v_x}, \quad \tan(\theta_r) = \frac{v_y - l_r\dot{\psi}}{v_x}. \tag{3}$$

As detailed in [3], the lateral tyre forces are proportional to the side-slip angle if the angles are small. Therefore, the lateral forces are calculated as

$$F_f = 2C_f(\delta - \theta_f), \quad F_r = 2C_r(-\theta_r), \tag{4}$$

where C_f and C_r are the front and rear tyre cornering stiffness, respectively.

We define a new variable β as

$$\beta = \frac{v_y}{v_x},$$

which describes the ratio between the lateral velocity and the longitudinal velocity. Using the new variable β and substituting (3) and (4) into the equations (1)-(2), the lateral dynamics of the vehicle can be rewritten as

$$\begin{aligned}\dot{\beta} =& \frac{2C_f}{mv_x}\delta - \dot{\psi} - \frac{2C_f}{mv_x}\arctan(\beta + \frac{l_f\dot{\psi}}{v_x}) \\ & - \frac{2C_r}{mv_x}\arctan(\beta - \frac{l_r\dot{\psi}}{v_x}), \\ \ddot{\psi} =& \frac{2C_f l_f}{I_z}\delta - \frac{2C_f l_f}{I_z}\arctan(\beta + \frac{l_f\dot{\psi}}{v_x}) \\ & + \frac{2C_r l_r}{I_z}\arctan(\beta - \frac{l_f\dot{\psi}}{v_x}),\end{aligned} \tag{5}$$

where the steering angle δ is the "input" signal.

Note that the steering angle cannot be controlled directly in a car. Instead, it is controlled by the steering torque. The dynamics of the steering system is given by the equation

$$J_s\ddot{\delta}_d + B_u\dot{\delta}_d = T_c - T_s, \tag{6}$$

where $\delta_d = \delta R_s$, R_s is the reduction ratio of the steering system, and J_s and B_u represent the moment of inertia and the damping coefficient of the steering system, respectively. T_c is the control input, while T_s is the self-aligning moment and is calculated as

$$T_s = -\frac{2C_f\eta_t}{R_s}\beta - \frac{2C_f l_f\eta_t}{R_s v_x}\dot{\psi} + \frac{2C_f\eta_t}{R_s^2}\delta_d. \tag{7}$$

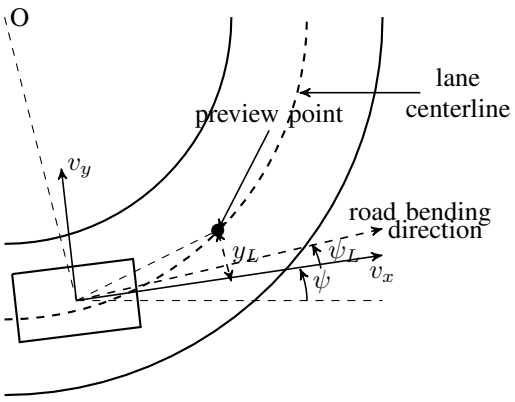

Fig. 2: Graphical Definitions of Variables y_L and ψ_L in Lane Keeping Cases.

In trajectory tracking (lane keeping) cases, two additional variables are used to describe the relationship between the vehicle and the reference trajectory (central line of the lane). They are the lateral deviation y_L and the heading error ψ_L. Their dynamics can be described by the equations

$$\begin{aligned}\dot{y}_L =& v_x\beta + T_p v_x\dot{\psi} + v_x\psi_L,\\ \dot{\psi}_L =& \dot{\psi} - v_x\rho,\end{aligned} \tag{8}$$

where ρ denotes the curvature of the reference trajectory (lane curvature). Note that the graphical definitions of the variables are illustrated in Fig. 2.

Definition 1: The signal $\rho(t)$ is said to be "feasible" if and only if there exist functions $\beta(t), \dot{\psi}(t), \delta(t), \dot{\delta}(t), y_L(t), \psi_L(t)$ and $T_c(t)$ such that the equations (5)-(6)-(7)-(8) hold for all $t \geq 0$.

Suppose $\rho(t)$ is feasible and v_x is a given positive constant. Then the references for the variables $\beta(t), \dot{\psi}(t), \delta(t), y_L(t), \psi_L(t), T_c(t)$ satisfy the equations

$$\begin{aligned}\dot{\beta}_r =& \frac{2C_f}{mv_x}\delta_r - \dot{\psi}_r - \frac{2C_f}{mv_x}\arctan(\beta_r + \frac{l_f\dot{\psi}_r}{v_x})\\ &- \frac{2C_r}{mv_x}\arctan(\beta - \frac{l_r\dot{\psi}}{v_x}),\\ \ddot{\psi}_r =& \frac{2C_f l_f}{I_z}\delta_r - \frac{2C_f l_f}{I_z}\arctan(\beta_r + \frac{l_f\dot{\psi}_r}{v_x})\\ &+ \frac{2C_r l_r}{I_z}\arctan(\beta_r - \frac{l_f\dot{\psi}_r}{v_x}),\\ \ddot{\delta}_r =& \frac{T_{c_r} - T_s - B_u R_s\dot{\delta}_r}{J_s R_s},\\ \dot{y}_{L_r} =& v_x\beta_r + T_p v_x\dot{\psi}_r + v_x\psi_{L_r},\\ \dot{\psi}_{L_r} =& \dot{\psi}_r - v_x\rho,\end{aligned} \tag{9}$$

where

$$T_s = -\frac{2C_f\eta_t}{R_s}\beta_r - \frac{2C_f l_f\eta_t}{R_s v_x}\dot{\psi}_r + \frac{2C_f\eta_t}{R_s}\delta_r.$$

The control problem for the lateral motion can then be formulated as follows.

Given the system (5)-(6)-(7)-(8) and the time history of the feasible road curvature $\rho(t)$, find (if possible) a feedback controller $T_c(t)$ such that the closed-loop system has the following properties.

P1) The control effort is bounded, *i.e.* $\exists\ \mathcal{B} > 0$ such that $|T_c(t)| \leq \mathcal{B}$ for all $t \geq 0$.

P2) The system state converges to its reference value, *i.e.*

$$\begin{aligned}\lim_{t\to\infty}&(\beta(t), \dot{\psi}(t), \delta(t), y_L(t), \psi_L(t)) -\\ &(\beta_r(t), \dot{\psi}_r(t), \delta_r(t), y_{L_r}(t), \psi_{L_r}(t)) = 0,\end{aligned}$$

where $\beta_r, \dot{\psi}_r, \delta_r, y_{L_r}$ and ψ_{L_r} are feasible reference signals.

P3) $\lim_{t\to\infty} T_c(t) - T_{c_r}(t) = 0$, where T_{c_r} is defined in (9).

III. PRELIMINARY THEOREMS

This section provides two basic results used to design the controller for the under-actuated nonlinear system (5).

Theorem 1: Consider a two dimensional system, the dynamics of which can be described by the equations

$$\begin{aligned}\dot{s}_1 =& q_{11}s_1 + p_1(s_2),\\ \dot{s}_2 =& p_2(s_1, s_2) + gu,\end{aligned} \tag{10}$$

where s_1 and s_2 are the states of the system, u is the control input, and $p_1 : \mathbb{R} \to \mathbb{R}$ and $p_2 : \mathbb{R}^2 \to \mathbb{R}$ denote two nonlinear mappings. Assume that

A1) $g \neq 0$;

A2) $q_{11} < 0$;

A3) The function $\dfrac{p_1(s_2)}{s_2}$ is continuous at $s_2 = 0$.

Then there exists a state-feedback controller $u(s_1, s_2)$ such that the zero equilibrium of the closed-loop-system is globally asymptotically stable. One such a choice is given by

$$u(s_1, s_2) = -\frac{ks_2 + s_1\dfrac{p_1(s_2)}{s_2} + p_2(s_1, s_2)}{g}, \tag{11}$$

for any $k > 0$.

Proof: Consider the Lyapunov function

$$L = \frac{1}{2}(s_1^2 + s_2^2).$$

Its time derivative along the trajectories of the closed-loop system is

$$\dot{L} = s_1[q_{11}s_1 + p_1(s_2)] + s_2[p_2(s_1, s_2) + gu].$$

By A3),

$$\dot{L} = q_{11}s_1^2 + s_2\left[s_1\frac{p_1(s_2)}{s_2} + p_2(s_1, s_2) + gu\right].$$

Substituting (11) into the above equation yields

$$\dot{L} = q_{11}s_1^2 - ks_2^2.$$

By A2) and the fact that $k > 0$ we conclude that

$$\dot{L} < 0$$

for all $(s_1, s_2) \neq (0, 0)$. Furthermore,

$$\dot{L} = 0 \Longleftrightarrow s_1 = s_2 = 0.$$

Therefore, the claim holds. ■

Theorem 2: Consider a system with two degrees-of-freedom, the dynamics of which is described by the equations

$$\begin{aligned} \dot{s}_1 =& a_{11}s_1 + a_{12}s_2 + f_1(s_2) + b_1u, \\ \dot{s}_2 =& a_{21}s_1 + a_{22}s_2 + f_2(s_2) + b_2u, \end{aligned} \tag{12}$$

with $s_1(t) \in \mathbb{R}, s_2(t) \in \mathbb{R}$ and $u(t) \in \mathbb{R}$. $a_{11}, a_{12}, a_{21}, a_{22}, b_1$ and b_2 are constant parameters, while $f_1(s_2)$ and $f_2(s_2)$ are continuous functions of s_2. Suppose that

H1) $\dfrac{f_1(s_2)}{s_2}$ and $\dfrac{f_2(s_2)}{s_2}$ are continuous at $s_2 = 0$;

H2) $b_2(b_1a_{21} - b_2a_{11}) > 0$.

Then there exists a state-feedback controller $u(s_1, s_2)$ such that the zero equilibrium of the closed-loop system is globally asymptotically stable. One such a choice is given by the feedback

$$\begin{aligned} u(s_1, s_2) =& \frac{-a_{21}s_1 - a_{22}s_2 - f_2(s_2) + b_1(b_1a_{21} - b_2a_{11})s_1}{b_2} \\ & - \frac{(b_1s_2 - b_2s_1)\left[b_1a_{22} - b_2a_{12} + b_1\dfrac{f_2(s_2)}{s_2}\right]}{b_2} \\ & - \frac{-(b_1s_2 - b_2s_1)b_2\dfrac{f_1(s_2)}{s_2} + ks_2}{b_2}, \end{aligned} \tag{13}$$

for any $k > 0$.

Proof: Define

$$\tilde{s}_1 \triangleq (b_1s_2 - b_2s_1)$$

and note that

$$\begin{aligned} \dot{\tilde{s}}_1 =& (b_1a_{21} - b_2a_{11})s_1 + (b_1a_{22} - b_2a_{12})s_2 \\ & + [b_1f_2(s_2) - b_2f_1(s_2)] \\ =& s_2\left[b_1a_{22} - b_2a_{12} + b_1\frac{f_2(s_2)}{s_2} - b_2\frac{f_1(s_2)}{s_2}\right] \\ & + (b_1a_{21} - b_2a_{11})s_1, \end{aligned}$$

hence

$$\begin{aligned} \dot{\tilde{s}}_1 =& q_{11}\tilde{s}_1 + p_1(s_2), \\ \dot{s}_2 =& p_2(\tilde{s}_1, s_2) + b_2u, \end{aligned}$$

where

$$\begin{aligned} q_{11} &= a_{11} - \frac{b_1}{b_2}a_{21}, \\ p_1(s_2) &= s_2\left[\begin{array}{c} b_1a_{22} - b_2a_{12} + b_1\dfrac{f_2(s_2)}{s_2} - b_2\dfrac{f_1(s_2)}{s_2} \\ +\dfrac{b_1}{b_2}(b_1a_{21} - b_2a_{11}) \end{array}\right], \\ p_2(\tilde{s}_1, s_2) &= a_{21}\frac{b_1s_2 - \tilde{s}_1}{b_2} + a_{22}s_2 + f_2(s_2). \end{aligned}$$

We now exploit Theorem 1, for which we need to check if A1) to A3) hold. To this end, note that

$$\text{H2)} \Longrightarrow \frac{b_2(b_1a_{21} - b_2a_{11})}{b_2^2} > 0 \Longrightarrow \frac{b_1}{b_2}a_{21} - a_{11} > 0.$$

Therefore, $q_{11} < 0$, *i.e.* A2) in Theorem 1 holds. Moreover, A1) and A3) are direct consequences of H2) and H1), respectively.

According to Theorem 1, the state-feedback control law

$$u(\tilde{s}_1, s_2) = -\frac{ks_2 + \tilde{s}_1\dfrac{p_1(s_2)}{s_2} + p_2(\tilde{s}_1, s_2)}{b_2}, \tag{14}$$

with $k > 0$, globally asymptotically stabilizes the zero equilibrium of system (12).

Rewriting the equation (14) with the variable s_1 and s_2 yields

$$\begin{aligned} u(s_1, s_2) =& -\frac{ks_2 + a_{21}\dfrac{b_1s_2 - b_1s_2 + b_2s_1}{b_2} + a_{22}s_2 + f_2(s_2)}{b_2} \\ & - \frac{(b_1s_2 - b_2s_1)(b_1a_{22} - b_2a_{12} + b_1\dfrac{f_2(s_2)}{s_2})}{b_2} \\ & + \frac{(b_1s_2 - b_2s_1)\left[b_2\dfrac{f_1(s_2)}{s_2} - \dfrac{b_1}{b_2}(b_1a_{21} - b_2a_{11})\right]}{b_2}, \end{aligned}$$

with $k > 0$, that is the control law (13). ■

IV. LATERAL CONTROL DESIGN FOR AUTONOMOUS VEHICLES

To design the lateral controller we regard the overall system as an inter connected system as depicted in Fig. 3. It is clear that the open-loop system contains three components, *i.e.* the 'Lateral Dynamics of the Vehicle', the 'Lane Keeping Dynamics' and the 'Steering System' together with the 'Self-Aligning Moment', of which the core subsystem is the "Lateral Dynamics of the Vehicle". This section gives a solution to the control problem stated in Section II.

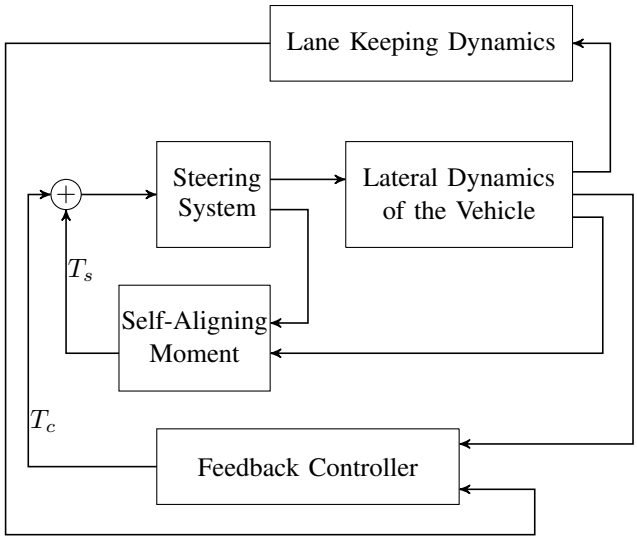

Fig. 3: Block Diagram of the System

A. Control Design for the Lateral Dynamics of the Vehicle

Consider the subsystem named as 'Lateral Dynamics of the Vehicle' in Fig. 3. This subsection studies how to design a controller for the nonlinear system (5) based on the preliminary results presented in Section III.

Define the variables x_1 and x_2 as

$$x_1 = \beta + \frac{l_f}{v_x}\dot{\psi}, \quad x_2 = \beta - \frac{l_r}{v_x}\dot{\psi}. \tag{15}$$

With the new variables the system (5) can then be rewritten as

$$\begin{aligned}
\dot{x}_1 =& -\frac{v_x}{l_f+l_r}x_1 + \frac{v_x}{l_f+l_r}x_2 + (\frac{2C_r l_r l_f}{I_z v_x} - \frac{2C_r}{m v_x})\arctan x_2 \\
&+ (\frac{2C_f l_f^2}{I_z v_x} + \frac{2C_f}{m v_x})(\delta - \arctan x_1), \\
\dot{x}_2 =& -\frac{v_x}{l_f+l_r}x_1 + \frac{v_x}{l_f+l_r}x_2 - (\frac{2C_r l_r^2}{I_z v_x} + \frac{2C_r}{m v_x})\arctan x_2 \\
&+ (\frac{2C_f}{m v_x} - \frac{2C_f l_f l_r}{I_z v_x})(\delta - \arctan x_1).
\end{aligned} \tag{16}$$

Regarding $(\delta - \arctan x_1)$ as an auxiliary input signal $\tilde{\delta}$, the system (16) can be rewritten in the form studied in Theorem 2 as

$$\begin{aligned}
\dot{x}_1 =& a_{11}x_1 + a_{12}x_2 + f_1(x_2) + b_1\tilde{\delta}, \\
\dot{x}_2 =& a_{21}x_1 + a_{22}x_2 + f_2(x_2) + b_2\tilde{\delta},
\end{aligned} \tag{17}$$

where

$$\begin{aligned}
a_{11} = a_{21} = -a_{12} = -a_{22} = -\frac{v_x}{l_f+l_r}, \\
b_1 = \frac{2C_f l_f^2}{I_z v_x} + \frac{2C_f}{m v_x}, \quad b_2 = \frac{2C_f}{m v_x} - \frac{2C_f l_f l_r}{I_z v_x}, \\
f_1(x_2) = (\frac{2C_r l_r l_f}{I_z v_x} - \frac{2C_r}{m v_x})\arctan x_2, \\
f_2(x_2) = (\frac{2C_r l_r^2}{I_z v_x} + \frac{2C_r}{m v_x})\arctan x_2.
\end{aligned}$$

Note that $b_1 > 0$ and $a_{11} = a_{21} < 0$.

Assumption 2: For typical values of car parameters $b_2 < 0$.

By Assumption 2 and the previous analysis on the signs of the parameters a_{11}, a_{21} and b_1 in (17), H2) in Theorem 2 holds. In addition, the function $\frac{\arctan x}{x}$ is continuous at $x = 0$, indicating that H1) of Theorem 2 holds.

According to Theorem 2, there exists a state-feedback controller $\tilde{\delta}(x_1, x_2)$ such that the zero equilibrium of the closed-loop system is globally asymptotically stable. One choice of $\tilde{\delta}(x_1, x_2)$ is given by

$$\begin{aligned}
\tilde{\delta} =& \frac{-a_{21}x_1 - a_{22}x_2 - f_2(x_2) + b_1(b_1 a_{21} - b_2 a_{11})x_1}{b_2} \\
&- \frac{(b_1 x_2 - b_2 x_1)\left[b_1 a_{22} - b_2 a_{12} + b_1 \dfrac{f_2(x_2)}{x_2}\right]}{b_2} \\
&- \frac{-(b_1 x_2 - b_2 x_1) b_2 \dfrac{f_1(x_2)}{x_2} + k_1 x_2}{b_2},
\end{aligned} \tag{18}$$

where $a_{11}, a_{12}, a_{21}, a_{22}, b_1, b_2, f_1(x_2)$ and $f_2(x_2)$ are defined in (17) and $k_1 > 0$.

Lemma 1: Consider the system (5) with the feedback controller $\delta = \tilde{\delta} + \arctan x_1$, where $\tilde{\delta}$ is given by (18) and x_1 and x_2 are defined in (15). The origin is a globally asymptotically stable equilibrium.

Proof: It is a direct consequence of Theorem 2. ■

B. Control Design for the Overall System

In this subsection we provide a control design for the overall system (5)-(6)-(7)-(8) in the case in which $\rho(t) = 0$ for all $t \geq 0$. In such a case $(\beta, \psi, \delta, y_L, \psi_L) = (0, 0, 0, 0, 0)$ is an equilibrium of the system (5)-(6)-(7)-(8), hence we define the reference trajectory as

$$\beta_r(t) = \dot{\psi}_r(t) = \delta_r(t) = \dot{\delta}_r(t) = y_{L_r}(t) = \psi_{L_r}(t) = 0,$$

for all $t \geq 0$.

Definition 2: Let $\phi(x) : \mathbb{R} \to \mathbb{R}$ be defined as

$$\phi(x) = \begin{cases}
1, & \text{if } x > \sqrt{2}, \\
\sqrt{1 - (\sqrt{2} - x)^2}, & \text{if } \frac{\sqrt{2}}{2} < x \leq \sqrt{2}, \\
x, & \text{if } -\frac{\sqrt{2}}{2} \leq x \leq \frac{\sqrt{2}}{2}, \\
-\sqrt{1 - (\sqrt{2} - x)^2}, & \text{if } -\sqrt{2} \leq x < -\frac{\sqrt{2}}{2}, \\
-1, & \text{if } x < -\sqrt{2}.
\end{cases}$$

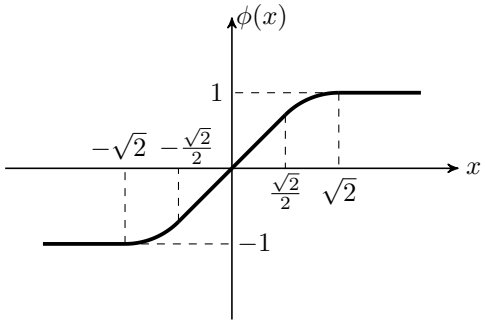

Fig. 4: The graph of the function $\phi(x)$ in Definition 2.

Fig. 4 illustrates the graph of the function $\phi(x)$. Note that $\phi(x)$ is twice differentiable.

On the basis of the control design for feedforward systems proposed in [21], we can derive the following result.

Lemma 2: Consider the lateral dynamics of the vehicle (5) together with the lane keeping dynamics (8). There exists $\kappa_1^* > 0, \kappa_2^* > 0, \epsilon_1^* > 0$ and $\epsilon_2^* > 0$ such that for any $\kappa_1 \in (0, \kappa_1^*), \kappa_2 \in (0, \kappa_2^*), \epsilon_1 \in (0, \epsilon_1^*)$ and $\epsilon_2 \in (0, \epsilon_2^*)$ the zero equilibrium of the closed-loop system (5)-(8) with the controller

$$\delta = \delta^* = \tilde{\delta} + \arctan x_1 - \epsilon_1 \phi(\frac{\kappa_1}{\epsilon_1}\psi_L) - \epsilon_2 \phi(\frac{\kappa_2}{\epsilon_2} y_L) \tag{19}$$

where $\tilde{\delta}$ and x_1 are defined in (18) and (15), respectively, is globally asymptotically stable.

Proof: In the case $\rho = 0$, the lane keeping dynamics described by the equations (8) are functions of the variables β and $\dot{\psi}$. Based on the relationship between the variables (x_1, x_2) and the variables $(\beta, \dot{\psi})$ given in (15), the system (8) can be rewritten as

$$\begin{aligned} \dot{y}_L =& v_x(\frac{l_r}{l_f + l_r} x_1 + \frac{l_f}{l_f + l_r} x_2) + v_x \psi_L, \\ &+ T_p v_x (\frac{v_x}{l_f + l_r} x_1 - \frac{v_x}{l_f + l_r} x_2) \\ \dot{\psi}_L =& \frac{v_x}{l_f + l_r} x_1 - \frac{v_x}{l_f + l_r} x_2, \end{aligned} \tag{20}$$

The linear approximation of the system (16) at the zero equilibrium point can be written as

$$\dot{x} = Fx + \begin{bmatrix} b_1 \\ b_2 \end{bmatrix} \tilde{\delta},$$

where

$$F = \begin{bmatrix} a_{11} & a_{12} + \dfrac{2C_r l_r l_f}{I_z v_x} - \dfrac{2C_r}{m v_x} \\ a_{21} & a_{22} + \dfrac{2C_r l_r^2}{I_z v_x} + \dfrac{2C_r}{m v_x} \end{bmatrix}.$$

Since the zero equilibrium of the system (16) with the control law (18) is globally asymptotically stable, the zero equilibrium of the closed-loop system (16)-(19)-(20) is globally asymptotically stable by applying Proposition 1 in [21] twice, hence the claim. ■

Note that the signal δ^* calculated in (19) is smooth and twice differentiable.

Finally, based on the back-stepping technique in [22], we obtain a control law for the overall system.

Theorem 3: Let $\rho(t) = 0$. Consider the system (5)-(6)-(7)-(8) with the controller

$$\begin{aligned} T_c =& T_s + J_s R_s [\ddot{\delta}^* - k_2(\dot{\delta} - \dot{\delta}^*)] + B_u R_s \dot{\delta} \\ &- k_3[\dot{\delta} - \dot{\delta}^* + k_2(\dot{\delta} - \dot{\delta}^*)] \\ =& -\frac{2C_f \eta_t}{R_s}\beta - \frac{2C_f l_f \eta_t}{R_s v_x}\dot{\psi} + \frac{2C_f \eta_t}{R_s}\delta + B_u R_s \dot{\delta} \\ &+ J_s R_s [\ddot{\delta}^* - k_2(\dot{\delta} - \dot{\delta}^*)] - k_3[\dot{\delta} - \dot{\delta}^* + k_2(\dot{\delta} - \dot{\delta}^*)], \end{aligned} \tag{21}$$

where δ^* is calculated in (19). Then the zero equilibrium of the closed-loop system is globally asymptotically stable.

Proof: The overall system can be written as

$$\begin{aligned} \dot{s} &= f_s(s) + g_s(s)\delta, \\ \ddot{\delta} &= \frac{T_c - T_s}{R_s J_s} - \frac{B_u}{J_s}\dot{\delta}, \end{aligned}$$

where $s = [\beta, \dot{\psi}, y_L, \psi_L]^T$, $f_s : \mathbb{R}^4 \to \mathbb{R}^4$ and $g_s : \mathbb{R}^4 \to \mathbb{R}^4$. Lemma 2 holds, hence the zero equilibrium of the subsystem

$$\dot{s} = f_s(s) + g_s(s)\delta^*(s)$$

is globally asymptotically stable and the corresponding Lyapunov function is $L(s)$. Using two steps of the back-stepping technique, we can prove that the controller (21) is globally asymptotically stabilizes the zero equilibrium of the system (5)-(6)-(7)-(8), hence the claim. ■

C. State-Feedback Tracking Control Design for the Overall System

This subsection discusses the lateral control design for the overall system (5)-(6)-(7)-(8) with non-zero, but feasible, road curvature $\rho(t)$. We say that $\rho(t)$ is feasible if $\beta_r, \dot{\psi}_r, \delta_r, y_{L_r}, \psi_{L_r}$ and T_{c_r} exist, where T_{c_r} denotes the reference control input.

Define the augmented reference signals x_{1r} and x_{2r} as

$$x_{1r} = \beta_r + \frac{l_f}{v_x}\dot{\psi}_r, \quad x_{2r} = \beta_r - \frac{l_r}{v_x}\dot{\psi}_r,$$

and the error signals x_{1e} and x_{2e} as

$$x_{1e} = x_1 - x_{1r}, \quad x_{2e} = x_2 - x_{2r}.$$

Based on (17) it is easy to derive the equations

$$\begin{aligned} \dot{x}_{1e} =& a_{11}x_{1e} + a_{12}x_{2e} + f_1(x_2) - f_1(x_{2r}) + b_1\tilde{\delta}_e, \\ \dot{x}_{2e} =& a_{21}x_{1e} + a_{22}x_{2e} + f_2(x_2) - f_2(x_{2r}) + b_2\tilde{\delta}_e, \end{aligned} \tag{22}$$

where $a_{11}, a_{12}, a_{21}, a_{22}, b_1, b_2, f_1(x_2)$ and $f_2(x_2)$ have the same definitions as those in (17). Moreover,

$$\tilde{\delta}_e = \delta - \arctan x_1 - \delta_r + \arctan x_{1r}.$$

Assumption 3: Assume that $x_2(t)x_{2r}(t) > -1$ for all $t \geq 0$.

Note that the above assumption holds in typical driving scenarios since the magnitudes of x_2 and x_{2r} are small.

Assumption 3 indicates that

$$\begin{aligned}\arctan x_2 - \arctan x_{2r} =& \arctan \frac{x_2 - x_{2r}}{1 + x_2 x_{2r}} \\ =& \arctan \frac{x_{2e}}{1 + x_2 x_{2r}}.\end{aligned}$$

Therefore

$$\begin{aligned}h_1(x_{2e}) \triangleq& f_1(x_2) - f_1(x_{2r}) \\ =& (\frac{2C_r l_r l_f}{I_z v_x} - \frac{2C_r}{m v_x}) \arctan \frac{x_{2e}}{1 + x_2 x_{2r}}, \\ h_2(x_{2e}) \triangleq& f_2(x_2) - f_2(x_{2r}) \\ =& (\frac{2C_r l_r^2}{I_z v_x} + \frac{2C_r}{m v_x}) \arctan \frac{x_{2e}}{1 + x_2 x_{2r}}.\end{aligned} \tag{23}$$

Hence, the system (22) satisfies all the hypothesis (*i.e.* H1 and H2) of Theorem 2.

Theorem 4: Consider the system (5)-(6)-(7)-(8) controlled by the feedback controller

$$\begin{aligned}T_c =& T_{c_r} - \frac{2C_f \eta_t}{R_s}\beta_e - \frac{2C_f l_f \eta_t}{R_s v_x}\dot{\psi}_e + \frac{2C_f \eta_t}{R_s}\delta_e + B_u R_s \dot{\delta}_e \\ &+ J_s R_s [\ddot{\delta}_e^* - k_2(\dot{\delta}_e - \dot{\delta}_e^*)] - k_3[\dot{\delta}_e - \dot{\delta}_e^* + k_2(\dot{\delta}_e - \dot{\delta}_e^*)],\end{aligned} \tag{24}$$

where

$$\begin{aligned}\delta_e^* = \tilde{\delta}_e + \arctan x_{1e} - \epsilon_1 \phi_e(\frac{\kappa_1}{\epsilon_1}\psi_{L_e}) - \epsilon_2 \phi(\frac{\kappa_2}{\epsilon_2} y_{L_e}), \\ \delta_e = \delta - \delta_r, \quad \beta_e = \beta - \beta_r, \quad \dot{\psi}_e = \dot{\psi} - \dot{\psi}_r,\end{aligned}$$

with

$$\begin{aligned}\tilde{\delta}_e =& \frac{-a_{21}x_{1e} - a_{22}x_{2e} - h_2(x_{2_e}) + b_1(b_1 a_{21} - b_2 a_{11})x_{1e}}{b_2} \\ &- \frac{(b_1 x_{2e} - b_2 x_{1e})\left[b_1 a_{22} - b_2 a_{12} + b_1 \dfrac{h_2(x_{2e})}{x_{2e}}\right]}{b_2} \\ &- \frac{-(b_1 x_{2e} - b_2 x_{1e}) b_2 \dfrac{h_1(x_{2e})}{x_{2e}} + k_1 x_{2e}}{b_2},\end{aligned}$$

$y_{L_e} = y_L - y_{L_r}$ and $\psi_{L_e} = \psi_L - \psi_{L_r}$. $h_1(x_{2e})$ and $h_2(x_{2e})$ are defined in (23) and k_i for all $i \in \{1, 2, 3\}$ are positive constants. Suppose that the reference trajectory $(\beta_r, \dot{\psi}_r, \delta_r, y_{L_r}, \psi_{L_r})$ is given and the road curvature $\rho(t)$ is feasible. In addition, we assume that Assumptions 1 to 3 hold. Then there exists $\kappa_1^* > 0, \kappa_2^* > 0, \epsilon_1^* > 0$ and $\epsilon_2^* > 0$ such that for any $\kappa_1 \in (0, \kappa_1^*), \kappa_2 \in (0, \kappa_2^*), \epsilon_1 \in (0, \epsilon_1^*)$ and $\epsilon_2 \in (0, \epsilon_2^*)$ the closed-loop system (5)-(6)-(7)-(8)-(24) has the following properties.

i) The tracking error converges to zero, *i.e.*

$$\lim_{t\to\infty}(y_L(t) - y_{L_r}(t)) = \lim_{t\to\infty}(\psi_L(t) - \psi_{L_r}(t)) = 0,$$

$$\lim_{t\to\infty}(\beta(t) - \beta r(t)) = \lim_{t\to\infty}(\dot{\psi}(t) - \dot{\psi}_r(t)) = 0.$$

ii) The control input is bounded, *i.e.* there exists a positive $\mathcal{T}$ such that $|T_c(t)| < \mathcal{T}$ for all $t \geq 0$.

Proof: According to the previous analysis, the system (22) meets all the hypothesis (*i.e.* H1 and H2) stated in Theorem 2. Similarly to the proof given in Subsection IV-B, Property i) holds due to Theorem 2, Proposition 1 stated in [21] and the back-stepping method detailed in [22].

Property ii) is a direct consequence of the definition of T_c given in (24). ■

Remark 1: Even though the controller is designed for lane keeping cases, it can also be used to change lanes. In lane changing cases a path planner in the outer loop has to generate a feasible reference trajectory which is then tracked by the car with the established lateral controller (24). Note that the path planning algorithm is not studied in the paper.

V. SIMULATION RESULTS AND ANALYSIS

This section discusses three case studies: uniform circular motion, tortuous path tracking and spiral tracking, to demonstrate the effectiveness of the developed control law. The cases are simulated by MATLAB SIMULINK and the results show that the established feedback controller is fast and effective in tracking reference trajectories with time-varying curvature. Note that in all the three cases we assume that the car is driven at a constant forward speed $v_x = 10\ m/s$. In addition, the parameter values for the car in all the simulations are given in Table I.

TABLE I: Vehicle Parameters

η	0.15	B_u	2.5	I_z	1500
C_f	170390	C_r	195940	J_s	0.05
l_f	1.48	l_r	1.12	m	1625
R_s	12				

A. Driver Model

To compare the performance of the feedback controller established in the paper with that of typical drivers we use the simplified two-level driver model developed in [23]. The model is a multi-input single-output model based on the observation of a far point and a near point, corresponding to θ_{far} and θ_{near} in Fig. 5, respectively. The visual far angle θ_{far} can be approximately calculated as

$$\theta_{far} \approx D\rho.$$

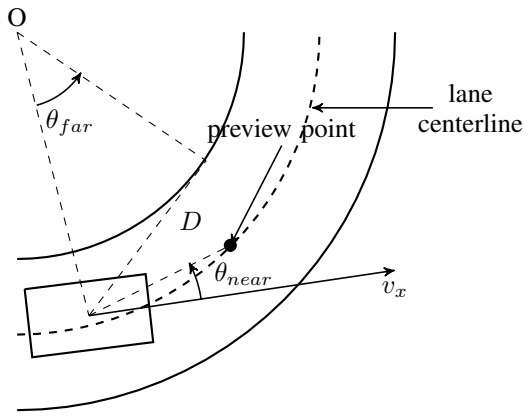

Fig. 5: Visual Angle Definitions in Driving Scenarios.

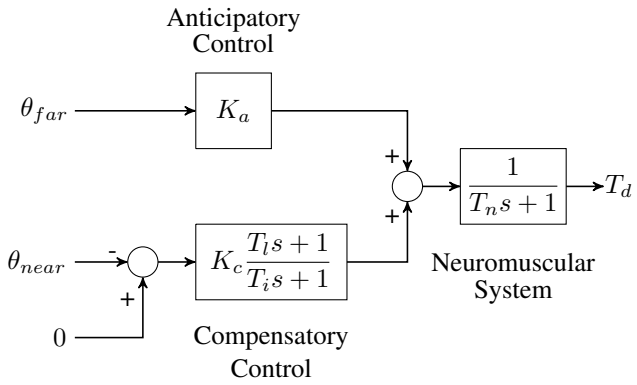

Fig. 6: Simplified Two-Level Driver Model.

In addition, the preview distance is defined as

$$x_L = v_x T_p,$$

where T_p is the driver's preview time. Therefore, the visual near angle θ_{near} is calculated as

$$\theta_{near} = \frac{y_L}{x_L} = \frac{y_L}{v_x T_p},$$

where y_L represent the lateral deviation, *i.e.* one of the states in the system (8).

The block diagram of the driver model is depicted in Fig. 6, where T_l and T_i denote the lead and lag time constants of the transfer function representing the compensatory steering control of the driver, respectively, while T_n represent the constant neuromuscular lag time of the driver. Furthermore, K_a and K_c describe the anticipatory control of the driver and the proportional gain of the driver with respect to the visual near angular error, respectively. The parameter values of the driver model representing typical drivers are given in Table II, from [23].

TABLE II: Typical Parameter Values for the Driver Model

T_l	T_i	T_n	D	T_p	K_a	K_c
1.16	0.14	0.11	15	2	56.97	36.13

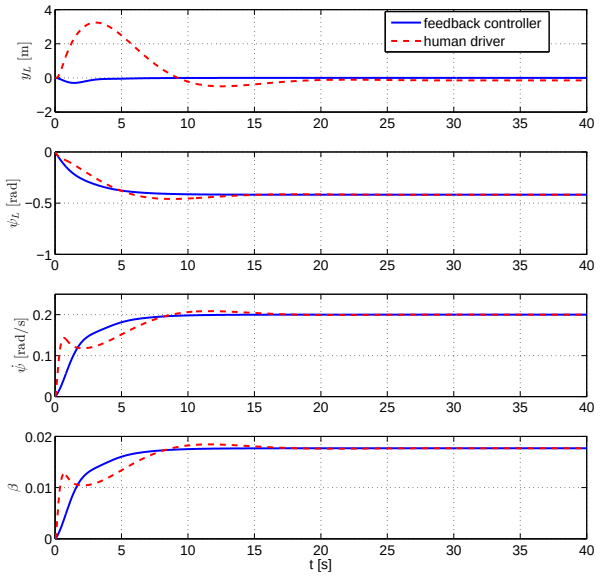

Fig. 7: Uniform Circular Motion. Time histories of the lateral deviation y_L, heading error ψ_L, yaw rate $\dot{\psi}$ and the ratio between the lateral speed and the longitudinal speed β for the system (5)-(6)-(7)-(8) with the feedback controller (24) and with a typical human driver.

In the following case studies we provide a comparison of simulation results between the performances of the closed-loop system with the state-feedback controller and with the typical driver.

B. Uniform Circular Motion

In this case study we assume that the curvature of the trajectory is constant, *i.e.* $\rho(t) = 0.02$ for all $t \geq 0$. In other words, the reference motion of the car is a uniform circular motion. Note that in the case study we assume that the reference trajectory changes suddenly from a straight line to a circle with radius equal to $50\ m$. This is different from the case in which the reference path is a straight line connected smoothly with a circle, because the human driver would start turning the steering wheel before entering the circular lane.

Simulation results are displayed in Fig. 7, in which the performance of the feedback controller and the modeled human driver are represented by the blue, solid line and the red, dashed line, respectively. Since all the four key variables related to the lateral dynamics of the vehicle converge to their steady-state values, *i.e.* reference values, it is obvious that both the feedback controller (24) and the human driver are able to control the system (5)-(6)-(7)-(8). In addition, the car with either of the controllers is able to track the reference path exactly when the curvature of the path is constant. However, by comparing the simulation results for the variable y_L, it is clear that the response of the closed-loop system with the

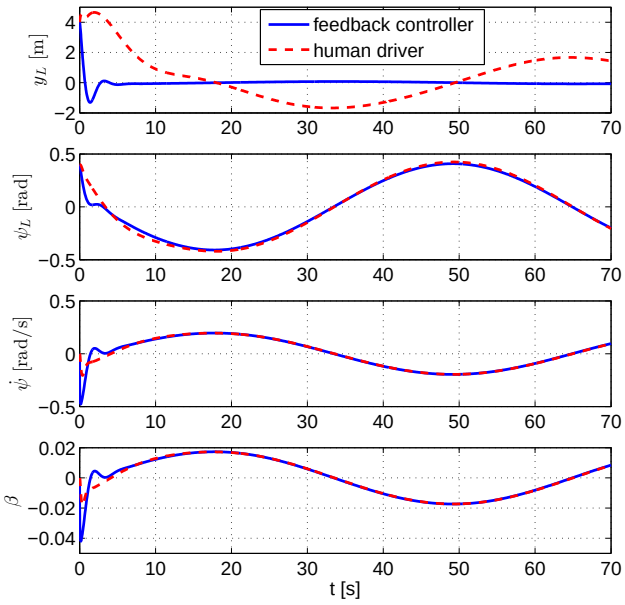

Fig. 8: Tortuous Path Tracking. Time histories of the lateral deviation y_L, heading error ψ_L, yaw rate $\dot{\psi}$ and the ratio between the lateral speed and the longitudinal speed β for the system (5)-(6)-(7)-(8) with the controller (24) and with a typical human driver.

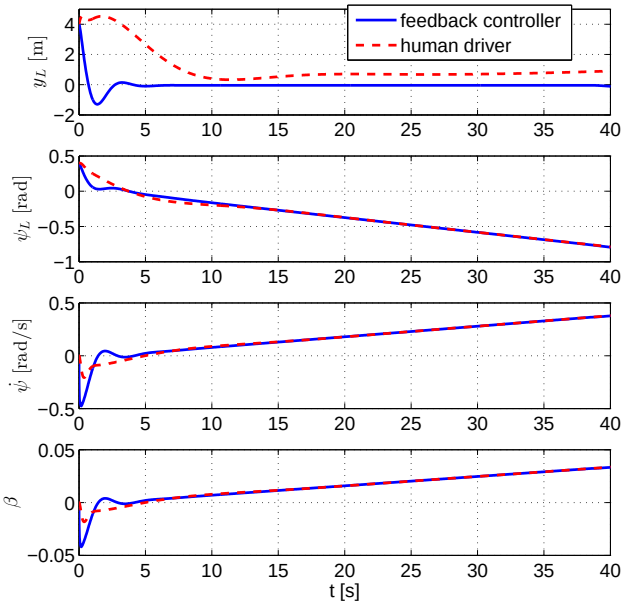

Fig. 9: Spiral Tracking. Time histories of the lateral deviation y_L, heading error ψ_L, yaw rate $\dot{\psi}$ and the ratio between the lateral speed and the longitudinal speed β for the system (5)-(6)-(7)-(8) with the controller (24) and with a typical human driver.

given feedback controller is much faster than that with the human driver. With the feedback controller (24) the lateral deviation is almost zero within 4 s, while the settling time for the closed-loop system with the human driver is about 20 s. In addition, the maximum lateral deviation is reduced from 3.2 m to 0.3 m by using the feedback controller.

C. Tortuous Path Tracking

In this case study the reference trajectory is a winding and tortuous path, with the curvature of the reference path defined as

$$\rho(t) = 0.02\sin(0.1t), \forall t \geq 0.$$

Simulation results are displayed in Fig. 8. Unlike the previous case study, the car with the human driver is unable to track the given reference trajectory. In the case study, we assume that the initial lateral deviation and the initial yaw error are 4 m and 0.4 rad, respectively. With the feedback controller, the closed-loop system is able to settle down within 4 s, while with the human driver, the lateral deviation is nonzero even after 70 s. This demonstrates that the feedback controller (24) is much more effective when the curvature of the reference trajectory is not constant. Even though the differences between the time histories of the variables ψ_L, $\dot{\psi}$ and β for two closed-loop systems are small, the differences between the time histories of y_L are significant because in this case the dynamics of y_L is described by

$$\dot{y}_L = 10\beta + 20\dot{\psi} + 10\psi_L.$$

If we increase the constant longitudinal speed v_x, then the time histories of the variable y_L for two closed-loop systems would have even larger differences.

D. Spiral Tracking

This case studies the performance of the system (5)-(6)-(7)-(8) when the curvature of the reference track is defined as

$$\rho(t) = 0.001t, \forall\ 0 \leq t \leq 40.$$

In other words, the reference path is a spiral the radius of which reduces continuously and uniformly from $+\infty$ to 25 m. We assume that the initial lateral deviation and yaw error are 4 m and 0.4 rad, respectively. Fig. 9 shows the simulation results for this case.

By comparing the settling time for all the three cases, we find out that the settling time for the closed-loop system with the feedback controller is less than 4 s no matter what the reference is. In other words, the lateral deviation converges to zero regardless of the variation of the variable ρ, which is consistent with Theorem 4.

VI. CONCLUSIONS

We have solved the asymptotic stabilization problem for a class of nonlinear systems. The solution, together with backstepping and feed-forward ideas, can be used to develop a lateral controller for autonomous vehicles. We have proved that with the established controller the vehicle is able to track any "feasible" references at a constant speed and the lateral deviation converges to zero within a short period. Even though the control design is based on the lane-keeping case, it can also be applied to lane-changing and other cases by using proper path planning methods to generate a "feasible" reference trajectory that the car follows. In the future, we will devote our efforts to the robust control design of the lateral dynamics of the vehicle in the presence of disturbances and uncertainties. We also aim to implement the controller in a high-fidelity model using CarSim.

REFERENCES

[1] J. Perez, V. Milanes, and E. Onieva, "Combined longitudinal and lateral control for automated vehicle guidance," *Vehicle System Dynamics*, vol. 52, no. 2, pp. 261–279, 2014.

[2] S. Li, F. Gao, D. Cao, and K. Li, "Multiple-model switching control of vehicle longitudinal dynamics for platoon-level automation," *IEEE Trans. on Vehicular Technology*, vol. 65, no. 6, pp. 4480–4492, 2016.

[3] R. Rajamani, *Vehicle Dynamics and Control*. Springer US, 2012.

[4] H. Zhang and J. Wang, "Vehicle lateral dynamics control through afs/dyc and robust gain-scheduling approach," *IEEE Transactions on Vehicular Technology*, vol. 65, no. 1, pp. 489–494, 2016.

[5] G. Han, W. Fu, W. Wang, and Z. Wu, "The lateral tracking control for the intelligent vehicle based on adaptive pid neural network," *Sensors*, vol. 17, no. 6, 2017.

[6] J. Yang and N. Zheng, "An expert fuzzy controller for vehicle lateral control," in *Proc. of IEEE Annual Conference on Industrial Electronics*, 2007, pp. 880–885.

[7] X. Huang, H. Zhang, G. Zhang, and J. Wang, "Robust weighted gain-scheduling H_∞ vehicle lateral motion control with considerations of steering system backlash-type hysteresis," *IEEE Transactions on Control Systems Technology*, vol. 22, no. 5, pp. 1740–1753, 2014.

[8] C. Latrach, M. Kchaou, A. E. Hajjaji, and A. Rahbi, "Robust H_∞ fuzzy networked control for vehicle lateral dynamics," in *Proc. of IEEE Annual Conference on Intelligent Transportation Systems*, 2013, pp. 905–910.

[9] R. Wang, Y. Sun, M. Lin, and H. Zhang, "Research on bus roll stability control based on LQR," in *Proc. of International Conference on Intelligent Transportation, Big Data and Smart City*, 2015, pp. 622–625.

[10] S. Lee and C. Chung, "Predictive control with sliding mode for autonomous driving vehicle lateral maneuvering," in *Proc. of American Control Conference*, 2017, pp. 2998–3003.

[11] G. Tagne, R. Talj, and A. Charara, "Higher-order sliding mode control for lateral dynamics of autonomous vehicles, with experimental validation," in *Proc. of IEEE Intelligent Vehicles Symposium*, 2013, pp. 678–683.

[12] C. Hatipoglu, U. Ozguner, and K. Redmill, "Automated lane change controller design," *IEEE Transactions on Intelligent Transportation Systems*, vol. 4, no. 1, pp. 13–22, 2003.

[13] J. Jiang and A. Astolfi, "A lateral control assistant for the dynamic model of vehicles subject to state constraints," in *Proc. of IEEE Conference on Decision and Control*, Melbourne, Australia, 2017.

[14] B. Gutjahr, L. Gröll, and M. Werling, "Lateral vehicle trajectory optimization using constrained linear time-varying MPC," *IEEE Transactions on Intelligent Transportation Systems*, vol. 18, no. 6, pp. 1586–1595, 2017.

[15] J. Levinson, J. Askeland, J. Becker, J. Dolson, D. Held, S. Kammel, J. Kolter, D. Langer, O. Pink, V. Pratt, M. Sokolsky, G. Stanek, D. Stavens, A. Teichman, M. Werling, and S. Thrun, "Higher-order sliding mode control for lateral dynamics of autonomous vehicles, with experimental validation," in *Proc. of IEEE Intelligent Vehicles Symposium*, 2011, pp. 163–168.

[16] P. Falcone, F. Borrelli, J. Asgari, H. Tseng, and D. Hrovat, "Predictive active steering control for autonomous vehicle systems," *IEEE Transactions on Control Systems Technology*, vol. 15, no. 3, pp. 566–580, 2007.

[17] J. Ahmadi, A. Sedigh, and M. Kabganian, "Adaptive vehicle lateral-plane motion control using optimal tire friction forces with saturation limits consideration," *IEEE Transactions on Vehicular Technology*, vol. 58, no. 8, pp. 4098–4107, 2009.

[18] J. Ni, J. Hu, and C. Xiang, "Envelope control for four-wheel independently actuated autonomous ground vehicle through AFS/DYC integrated control," *IEEE Transactions on Vehicular Technology*, vol. PP, no. 99, pp. 1–1, 2017.

[19] S. Dominguez, A. Ali, G. Garcia, and P. Martinet, "Comparison of lateral controllers for autonomous vehicle: Experimental results," in *Proc. of IEEE Conference on Intelligent Transportation Systems*, 2016, pp. 1418–1423.

[20] G. Tagne, R. Talj, and A. Charara, "Design and comparison of robust nonlinear controllers for the lateral dynamics of intelligent vehicles," *IEEE Transactions on Intelligent Transportation Systems*, vol. 17, no. 3, pp. 796–809, 2016.

[21] G. Kaliora and A. Astolfi, "Nonlinear control of feedforward systems with bounded signals," *IEEE Transactions on Automatic Control*, vol. 49, no. 11, pp. 1975–1990, 2004.

[22] P. Kokotovic, "The joy of feedback: Nonlinear and adaptive," *IEEE Control Systems*, vol. 12, no. 3, pp. 7–17, 1992.

[23] C. Sentouh, P. Chevrel, F. Mars, and F. Claveau, "A sensorimotor driver model for steering control," in *Proc. of IEEE Conference on Systems, Man and Cybernetics*, 2009, pp. 2462–2467.

Jingjing Jiang was born in China. She received the B.Eng. Degree in Electrical and Electronic Engineering from the University of Birmingham, UK, and the Harbin Institute of Technology, China, in 2010, the M.Sc. degree in Control Systems with Department Prize for Outstanding Achievement from Imperial College London, UK, in 2011, and the Ph.D degree from Imperial College London, in 2016, with a Thesis on Shared-Control for Systems with Constraints. Since 2016 she has been with the Electrical and Electronic Engineering Department of Imperial College London, London (UK), where she is currently a research associate in the Control and Power Group. Her current research interests include driver assistance control and autonomous vehicle control design, control design of systems with constraints and human-in-the-loop.

Alessandro Astolfi (F' 2009) was born in Rome, Italy. He received the Bachelor Degree in Electrical Engineering from the University of Rome, Rome, in 1991, the M.Sc. in Information Theory and the Ph.D. (Hons.) with a Thesis on Discontinuous Stabilization of Nonholonomic Systems from ETH Zurich, Zrich, Switzerland, in 1995, and the Ph.D. degree on nonlinear robust control from the University of Rome in 1996. He has been with the Electrical and Electronic Engineering Department, Imperial College London, London, UK., since 1996, where he is currently a Professor of Nonlinear Control Theory and the Head of the Control and Power Group. He was an Associate Professor with Politecnico of Milano, Milan, Italy, from 1998 to 2003. He has also been a Professor at University of Rome Tor Vergata, Rome, since 2005. His current research interests include control theory and applications, with special emphasis for the problems of discontinuous stabilization, robust and adaptive control, observer design and model reduction. Dr. Astolfi, a Distinguished Member of the IEEE Control Systems Society (CSS), was a recipient of the IEEE CSS A. Ruberti Young Researcher Prize in 2007, and the IEEE CSS George S. Axelby Outstanding Paper Award in 2012.